ACS OMEGA

http://pubs.acs.org/journal/acsodf

Article

A Novel Molecular Approach for Enhancing the Safety of Ozone in Autohemotherapy and Insights into Heme Pocket Autoxidation of Hemoglobin

Ramin Naderi Beni, Zahra Hassani-Nejad Pirkouhi, Fouad Mehraban, and Arefeh Seyedarabi*

Cite This: *ACS Omega* 2023, 8, 20714−20729

Read Online

ACCESS | Metrics & More | Article Recommendations | Supporting Information

ABSTRACT: Major ozone autohemotherapy (MAH) is a popular clinical practice for treating a variety of pathological conditions due to the mild and controlled oxidative stress produced by the reaction of ozone gas with other biological components. Previous studies have shown that blood ozonation leads to structural changes in hemoglobin (Hb); therefore, in the present study, the molecular effects of ozonation on Hb of a healthy individual were assessed by ozonating whole blood samples with single doses of ozone at 40, 60, and 80 μg/mL or double doses of ozone at 20 + 20, 30 + 30, and 40 + 40 μg/mL ozone to investigate whether ozonating once versus twice (but with the same final ozone concentration) would have varying effects on Hb. Additionally, our study aimed to verify whether using a very high ozone concentration (80 + 80 μg/mL), despite mixing it with blood in two steps, would result in Hb autoxidation. The pH, oxygen partial pressure, and saturation percentage of the whole blood samples were measured through a venous blood gas test, and the purified Hb samples were analyzed using several techniques including intrinsic fluorescence, circular dichroism and UV−vis absorption spectroscopies, SDS-polyacrylamide gel electrophoresis, dynamic light scattering, and a zeta potential analyzer. Structural and sequence analyses were also used to study the Hb heme pocket autoxidation sites and the residues involved. The results showed that the oligomerization and instability of Hb can be reduced if the ozone concentration to be used in MAH is divided into two doses. Indeed, our study demonstrated that two-step ozonation with 20, 30, and 40 μg/mL of ozone instead of single-dose ozonation with 40, 60, and 80 μg/mL of ozone reduced the potential adverse effects of ozone on Hb including protein instability and oligomerization. Moreover, it was found that for certain residues, their orientation or displacement leads to the entry of excess water molecules into the heme moiety, which can contribute to Hb autoxidation. Additionally, the autoxidation rate was found to be higher in alpha globins compared to beta globins.

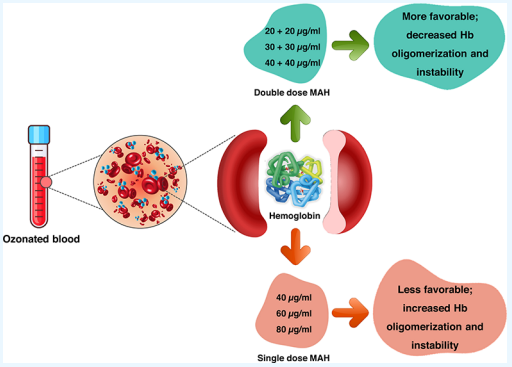

1. INTRODUCTION

Ozone gas is a colorless, water-soluble molecule composed of three atoms of oxygen (O_3) and is believed to have numerous therapeutic applications with an array of antiseptic properties.[1] The oxidant strength of ozone is the third highest after fluorine and persulfate.[2] In clinical settings, controlled and innocuous concentrations of oxygen (95−99%) and ozone (5−1%) are applied using a medical-grade ozone generator.[3] Typically, the ozone concentration ranges from 10 to 80 μg/mL, and although the majority of the mixture consists of oxygen, minor changes in ozone concentration can significantly alter the overall effect of ozone therapy.[4] Although the highest medical concentration of ozone is equivalent to 80 μg/mL, the use of higher concentrations (up to 160 μg/mL) has also been investigated in previous studies.[5,6]

Currently, ozone therapy is used as a complementary medical approach for treating a plethora of ailments including vascular and neurodegenerative diseases.[7] However, the long-term effect of ozone therapy merits further investigation as well as controlled and randomized clinical trials. Ozone therapy is known to modulate free radicals and antioxidant levels by inducing controlled and moderate oxidative stress.[7,8] Due to the fact that ozone has no receptors, its mechanism of action is indirect and is correlated to the activation of Nrf2 (nuclear factor erythroid 2-related factor 2) and protein synthesis pathways.[9] Once ozone enters the bloodstream, it reacts with polyunsaturated fatty acids (PUFAs) of the plasma membrane and leads to the formation of two secondary messengers: hydrogen peroxide (H_2O_2) and lipid ozonation products (LOPs).[10] The biological activity of ozone may be mediated by these messengers as they partake in signal transduction and increase the expression of

Received: February 26, 2023
Accepted: May 4, 2023
Published: May 26, 2023

casein kinase 2, which regulates the activity of Nrf2 through its phosphorylation. Activation of Nrf2 leads to the production of a set of antioxidant enzymes and free antioxidant response elements that can alleviate chronic oxidative stress caused by the underlying disease and protect cells from the harmful effects of oxidation and inflammation.[7,11,12] The effectiveness and the toxicity levels of ozone vary based on the strength of the oxidative stress; severe oxidative stress triggers nuclear transcriptional factor kappa B, which subsequently induces inflammatory responses, whereas Nrf2 is activated in moderate oxidative stress.[7,11]

Ozone has other applications in the medical field. For instance, a number of studies have shown that ozone exhibits bactericidal activity and can efficiently kill microorganisms such as *Staphylococcus aureus* (*S. aureus*), *Escherichia coli*, *Pseudomonas aeruginosa*, and *Enterococcus faecalis*, with 99.6% growth inhibition against *S. aureus*.[13,14] The bactericidal activity of ozone mostly relies on disrupting the integrity of bacterial cells through oxidizing its membrane proteins (glycoproteins and lipoproteins) and phospholipids, all of which will lead to an attenuation in the stability of the bacterial cell and interfere with its reproductive cycle.[11,15,16]

Currently, the most popular ozone therapy approach is known as major ozone autohemotherapy (MAH), also referred to as auto-hemotransfusion, in which a small volume of blood is drawn from the patient, mixed with a precise concentration of medical-grade ozone *ex vivo*, and then reinfused into the bloodstream of the patient.[11,17] Despite its advantages, ozone gas is toxic at concentrations higher than the therapeutic range, and its administration needs to be judiciously monitored by choosing the appropriate concentration, exposure time, and administration route. Moreover, the effect of ozone in MAH varies among individuals based on their plasma antioxidant levels, highlighting the importance of personalizing ozone therapy.[17,18] Hence, it is highly recommended to accurately assess the effect of different concentrations of ozone on whole blood samples of patients before initiating MAH.

Ozone can dissolve in aqueous environments and release its energy to hematic components[19] including hemoglobin (Hb), the most abundant heme-containing protein in the blood circulation. Additionally, ozone gas is found to accelerate autoxidation processes,[20] and previous studies have shown that the number of water molecules in the heme pocket as well as the presence and orientation of certain amino acids determines the rate of autoxidation in Hb.[21] Autoxidation of oxygen binding heme proteins is an inevitable phenomenon in which the heme-iron is oxidized from ferrous to ferric state and prevents the reversible binding of oxygen to Hb.[22] The Hb protein is inactivated when all of its iron atoms are autoxidized, which subsequently leads to hemin loss and denaturation of the apoglobin.[23] The Hb heme either can bind to oxygen (Oxy-Hb), carbon monoxide (CO-Hb), or water (Met-Hb) or can also be non-ligand-bound, which is referred to as deoxy-Hb. The autoxidized form of Hb is called Met-Hb, in which the sixth coordination position of the iron atom is occupied by a water molecule.[24] Additionally, the autoxidation rate and the oxygen binding affinity vary between alpha and beta globin chains of Hb, with the autoxidation rate being higher in the former because of the water molecules being already present in the proximity of the heme group of the alpha globin, whereas in the beta globin (specifically in human Hb), there is a valine (Val) residue at position 67 blocking the ligand binding site.[25,26] Furthermore, it has been reported that hemin loss is more likely to occur when water molecules gain entry to both distal and proximal portions of the heme pocket in Met-Hb, which increases the rate of oxidative stress.[27] Insights into the structural changes of Hb that promote autoxidation and eventual hemin loss are of great importance because they can pave the way for developing cardiovascular medications.[28]

Since ozone gas is a potent oxidizing agent, its reaction with proteins leads to ozonolysis of certain amino acids such as tryptophan (Trp), tyrosine (Tyr), and cysteine (Cys) and subsequently alters protein folding and binding abilities.[29] Additionally, previous research has established that ozonation leads to structural changes in Hb in a dose- and time-dependent manner,[18,30,31] and it has been set forth that autoxidation of Hb, which is unfavorable as it causes lipid oxidation,[32] is partly due to the presence of certain amino acids and their orientation around the heme group as well as the number of water molecules in the heme pocket.[21]

A previous study has shown that ozonating whole blood and saline-washed erythrocytes at concentrations of 20, 40, 80, and 160 μg/mL leads to serious damage to saline-washed erythrocytes, indicating that in the absence of potent plasma antioxidants, the erythrocytes are more prone to degradation.[5] In another study, the effect of ozone concentrations of 40, 80, and 160 μg/mL using an *in vitro* MAH method was evaluated on various blood parameters of aortic dissection patients, including free hemoglobin levels, to assess hemolysis and morphological alterations of erythrocytes in comparison to the nonozonated sample. The results revealed that exceeding the ozone concentration to 160 μg/mL increased the rate of malformation and morphological changes of erythrocyte samples in both patients and the control group.[6] Furthermore, similar results have been seen using ozone concentrations of 1 and 10 μg/mL for purified Hb versus whole blood samples, showing that in the purified Hb samples, more adverse structural changes were observed because of the absence of blood antioxidants, whereas the presence of antioxidants in the whole blood samples prevented major alterations in the Hb structure.[18] Additionally, in another study, it was seen that ozonating stored human blood with concentrations below 80 μg/mL did not adversely affect the heme binding to Hb, and hence, it was not toxic.[33] Interestingly, it was previously reported that alkalinity (due to the presence of carbonate and bicarbonate ions) influenced the conformation of Hb upon ozonation by reducing the rate of ozone decomposition. Moreover, Hb oligomerization was increased at a higher rate when using higher concentrations of ozone in samples where phosphate buffer was diluted with ion-free water.[31]

Table 1 summarizes the results of previous MAH studies and their corresponding effects on blood components. All of the reported studies had assessed the effect of MAH using a single dose of ozone at different concentrations. None of the studies had compared the effect of using a double dose of ozone versus a single dose, as reported in the present study.

Given the available literature and research conducted so far, in the present study, human nonozonated and ozonated Hb samples treated with either a single dose (40, 60, and 80 μg/mL) or double dose of ozone (20 + 20, 30 + 30, and 40 + 40 μg/mL) were analyzed using techniques such as intrinsic fluorescence, far- and near-circular dichroism, UV−vis absorption, SDS-polyacrylamide gel electrophoresis (SDS-PAGE), dynamic light scattering, as well as zeta potential to assess whether there will be any differences between the single-dose- and double-dose-ozonated Hb samples. This was done to determine if using the

https://doi.org/10.1021/acsomega.3c01288
ACS Omega 2023, 8, 20714−20729

Table 1. List of Previous MAH Studies and Their Corresponding Effects on Blood Components

Publication year	Ozone concentrations (μg/mL)	Method	Ozone exposure time	Samples	Results	Reference
2007	20, 40, 80, and 160	Single dose	10 min	Healthy human whole blood and saline-washed erythrocytes	Ozone causes serious damage to saline-washed erythrocytes.	5
2018	40, 80, and 160	Single dose	20 min	Blood of aortic dissection patients	Ozonation increases the levels of free Hb in samples ozonated at 80 and 160 μg/mL. An ozone concentration of 160 μg/mL leads to hemolysis and changes the erythrocyte morphology.	6
2018	1 (for purified Hb) and 10 (for whole blood)	Single dose	5 and 10 min (for whole blood); 10, 30, and 60 s (for purified Hb)	Whole blood and purified human Hb	The presence of antioxidants prevents Hb degradation.	18
2019	15, 35, and 55	Single dose	5 min	Nondiabetic individuals and type II diabetic patients	The ozone concentration in MAH should be personalized for each individual.	30
2020	55 and 80	Single dose	5 min	Purified human Hb in phosphate buffer and diluted versions with deionized, double distilled, and tap water	Alkalinity (the presence of carbonate and bicarbonate ions) can reduce the destructive oxidation effects of high ozone concentrations on Hb.	31
2012	30, 50, 70, and 80	Single dose	10 min	Stored healthy human blood	Ozone does not react with Hb iron, and ozone concentrations below 80 μg/mL are not toxic.	33

aforementioned method in MAH can potentially reduce the oligomerization and instability of Hb. Additionally, Hb samples ozonated with 80 + 80 μg/mL of ozone were also studied as a means to highlight the destructive effects of very high concentrations of ozone on human Hb (even when administered in two doses). Furthermore, the whole blood samples ozonated at concentrations of 40, 60, and 80 μg/mL were sent for venous blood gas (VBG) tests to determine variations in the pH, oxygen partial pressure, and saturation percentage values. The second part of this study involved identifying the Hb heme pocket residues that increase the autoxidation rate through using structural and sequence analyses and molecular visualization tools.

2. METHODS

2.1. Blood Collection and Ozonation. A volume of 40 mL of venous blood was collected from a healthy, 27-year-old nonsmoker male who provided consent for his participation in this study. Sodium citrate (4%) was used as anticoagulant, and the samples were divided into eight equal volumes: one was nonozonated (control); three were ozonated once with ozone concentrations of 40, 60, and 80 μg/mL; and the remaining samples were ozonated twice with ozone concentrations of 20, 30, 40, and 80 μg/mL. All ozonated samples were exposed to an ozone−oxygen gas mixture composed of 5% ozone and 95% oxygen for 5 min at a 1:1 volumetric ratio using a Gardina medical ozone generator (Figure 1).

2.2. Venous Blood Gas (VBG) Test. After blood collection and ozonation, the blood samples were sent to the Tehran Heart Center for VBG analysis using a MEDICA Easy Stat blood gas analyzer to measure the pH, partial pressure, and percent saturation of oxygen in the nonozonated and 40, 60 and, 80 μg/mL ozonated whole blood samples.

2.3. Hb Purification. The Hb of the nonozonated and ozonated samples was purified by a previously reported method.[18] Briefly, the blood samples were centrifuged at 850*g* for 20 min at 4 °C to remove the plasma components. The pellets were first washed with 0.9% NaCl isotonic saline solution and then with sodium phosphate buffer (200 mM, pH 7.4) three times, and finally, cold double distilled water was added to osmotically lyse the red blood cells. Subsequently, the samples were centrifuged at 20,000*g* for 20 min at 4 °C to remove membrane components. With the use of neutralized solid ammonium sulfate, the Hb solution was brought to 20% saturation, incubated for 15 min at 4 °C, and centrifuged at a speed of 18,000*g* for 60 min at 2 °C. The precipitate was discarded, and the samples were dialyzed in sodium phosphate buffer (50 mM, pH 7.4) for 24 h using 10 kDa molecular weight cutoff dialysis membranes.

2.4. Intrinsic Fluorescence Spectroscopy. Fluorescence emission spectra were measured using a spectrofluorometer (Varian, Cary Eclipse, Australia). The intrinsic fluorescence spectra of Hb were measured over a wavelength range of 300 to 400 nm using an excitation wavelength of 280 nm, corresponding to Tyr and Trp residues.

2.5. CD Measurements. CD measurements were carried out using an AVIV 215 spectropolarimeter (Aviv Associates, Lakewood, NJ, USA) with 50 mM phosphate buffer (pH 7.4) as blank and protein concentrations of 0.5 mg/mL for near-UV CD and 0.2 mg/mL for far-UV CD analyses. The samples were examined at 190−260 and 240−460 nm designated for far- and near-UV CD spectra, respectively. The results were plotted using ellipticity as a function of wavelength in nanometers.

https://doi.org/10.1021/acsomega.3c01288
ACS Omega 2023, 8, 20714−20729

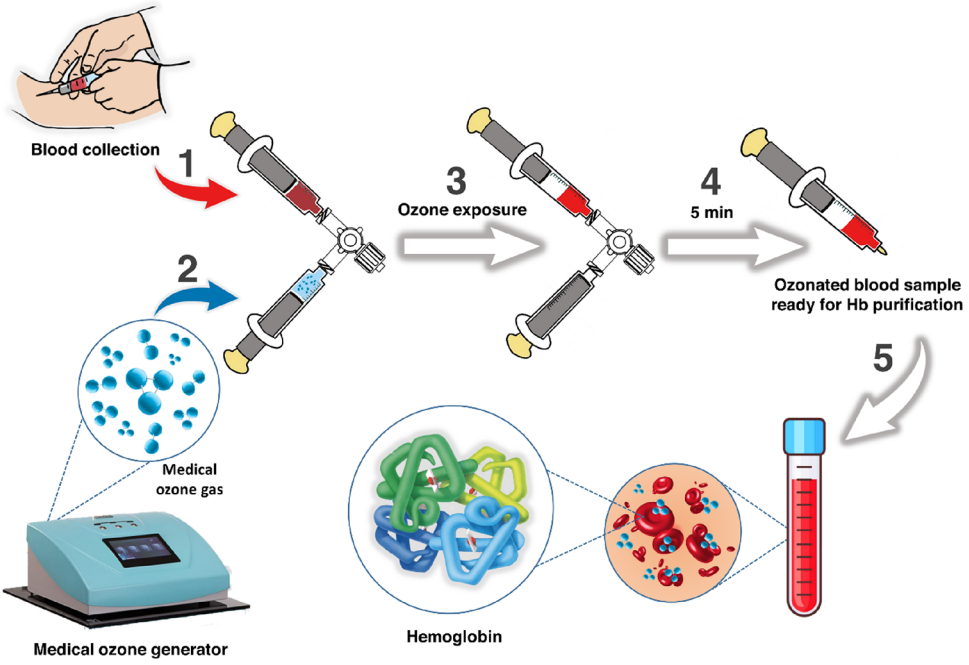

Figure 1. A schematic representation of blood collection and ozonation. Venous blood is collected (1), and the proper ozone concentration is obtained from a medical-grade ozone generator (2). The blood sample gets exposed to the ozone−oxygen gas mixture for 5 min at a 1:1 volumetric ratio (3 and 4), and the blood sample's color changes to a brighter red. For double-dose ozonation, steps 3 and 4 are repeated. Subsequently, the ozonated blood is ready for Hb purification (5).

2.6. UV−Vis Absorption Spectroscopy. The concentrations of the nonozonated and ozonated protein samples were estimated using absorption at 280 nm and the extinction coefficient $\varepsilon = 2.65\ dm^3\ g^{-1}\ cm^{-1}$. The absorbance and UV scan spectra of the nonozonated and ozonated samples were measured using a UV−visible spectrophotometer (Varian, Cary 100 Bio, Australia) at an absorbance of 280 nm and reported in the range of 200−700 nm.

2.7. SDS-PAGE. All samples were mixed with equal volumes of the loading buffer (0.05 M Tris−HCl, 2% SDS; 10% glycerol, and 0.1% bromophenol blue, pH 6.8) either with dithiothreitol (DTT) or without DTT, heated at 100 °C for 10 min, and loaded into an 18% SDS gel.

2.8. Dynamic Light Scattering and Zeta Potential. The hydrodynamic sizes and the surface charges of nonozonated and ozonated Hb samples were measured using a nanoparticle size analyzer (SZ-100-Horiba, Japan) dynamic light scattering instrument. Samples were loaded into disposable 1 cm optical path cuvettes. The refractive index of the protein was set to 1.59, and the absorption was set to 0.01 using a dispersion medium viscosity of 0.893 mPa·s and a refractive index of 1.33.

2.9. Bioinformatic Analysis. A protein BLAST search was done using the Hb sequence related to Caspian Sea sturgeon *Acipenser stellatus* (PDB ID: 6IYI) as reference, with evidence of heme oxidation. This structure had been previously determined by our group using macromolecular X-ray crystallography.[21] The PDB ID selection for alpha and beta globins was based on native (unmutated) and noncomplexed forms of Hb in different heme states (CO-Hb, deoxy-Hb, Met-Hb, and Oxy-Hb). Afterward, Chimera[34] and LigPlot[35] programs were used for detailed sequence and structural analyses.

3. RESULTS

3.1. Venous Blood Gas Analysis. The venous blood gas (VBG) test is designated for determining the acid−base status (pH) of the blood as well as the partial pressure of gases like oxygen (PO_2) and oxygen saturation (saO_2) levels.[36,37] The PO_2 levels signify the amount of oxygen gas dissolved in the blood, and the saO_2 level is a measure of the amount of oxygen bound to Hb in the red blood cells.[37] The VBG results of the whole blood samples are shown in Table 2. In the case of 60 and 80 μg/mL ozonated samples, the blood samples became more acidic (pH decreased), whereas in the 40 μg/mL ozonated sample, the pH did not change with respect to the nonozonated (control) sample. However, the PO_2 and saO_2 levels increased with increasing ozone concentration, which indicate an increase in dissolved oxygen and Oxy-Hb levels, respectively.

Table 2. VBG Test Results Showing the pH, PO_2, and saO_2 Status of Nonozonated (Control) and Ozonated Whole Blood Samples with Ozone Concentrations of 40, 60, and 80 μg/mL[a]

sample	pH	PO_2 (mmHg)	saO_2 (%)
control	7.41	46	82.9
40 μg/mL	7.41	82	96.3
60 μg/mL	7.38	283	99.9
80 μg/mL	7.37	288	99.9

[a]The first column shows the sample type, the second column indicates the sample pH, the third column displays the partial pressure of oxygen or the amount of oxygen dissolved in the blood in mmHg, and the fourth column shows the percent saturation of oxygen or the amount of oxygen bound to Hb.

3.2. Intrinsic Fluorescence Spectroscopy Results. Intrinsic fluorescence is a widely used method for studying the dynamics and conformational characteristics of proteins. The intrinsic fluorescence property of proteins is mainly due to the presence of aromatic residues such as Trp, Tyr, and phenylalanine (Phe), all of which are sensitive to the polarity of the

https://doi.org/10.1021/acsomega.3c01288
ACS Omega 2023, 8, 20714−20729

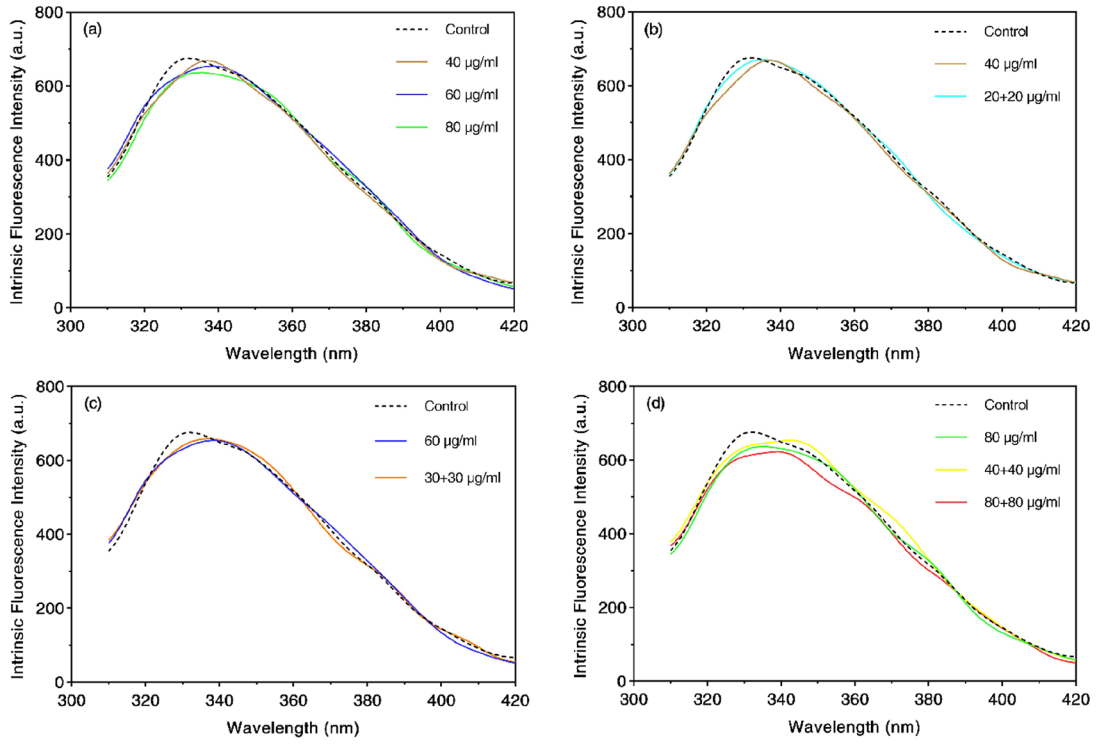

Figure 2. The intrinsic fluorescence spectral changes of ozonated and nonozonated Hb samples excited at λ_{ex} = 280 nm. (a) Fluorescence spectra of control and 40, 60, and 80 μg/mL ozonated samples. (b) Fluorescence spectra of control and 40 and 20 + 20 μg/mL ozonated samples. (c) Fluorescence spectra of control and 60 and 30 + 30 μg/mL ozonated samples. (d) Fluorescence spectra of control and 80 and 40 + 40 μg/mL ozonated samples plus the 80 + 80 μg/mL ozonated sample.

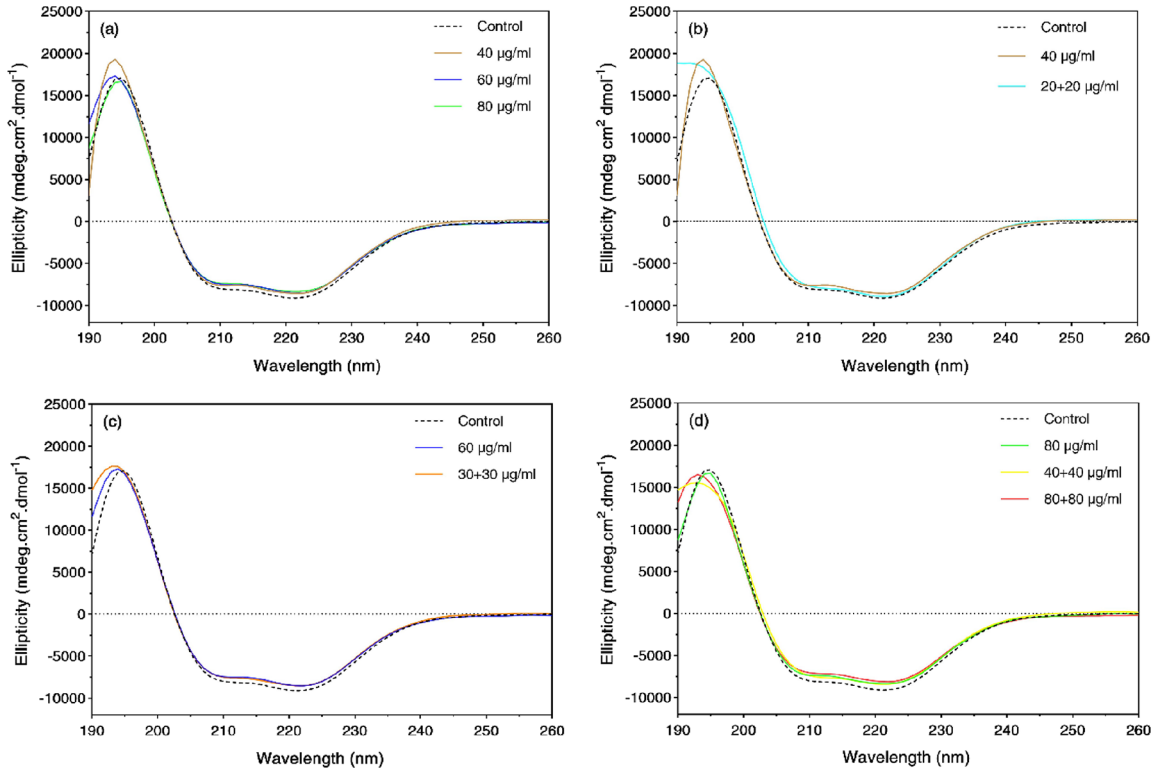

Figure 3. Far-UV CD spectral changes of ozonated and nonozonated Hb samples. (a) Far-UV spectra of control and 40, 60, and 80 μg/mL ozonated samples. (b) Far-UV spectra of control and 40 and 20 + 20 μg/mL ozonated samples. (c) Far-UV spectra of control and 60 and 30 + 30 μg/mL ozonated samples. (d) Far-UV spectra of control and 80, 40 + 40, and 80 + 80 μg/mL ozonated samples.

protein's local environment, and alterations in the surrounding microenvironment of these residues can lead to protein structural changes.[38] Figure 2 depicts the intrinsic fluorescence spectra of ozonated and nonozonated Hb samples. The

https://doi.org/10.1021/acsomega.3c01288
ACS Omega 2023, 8, 20714−20729

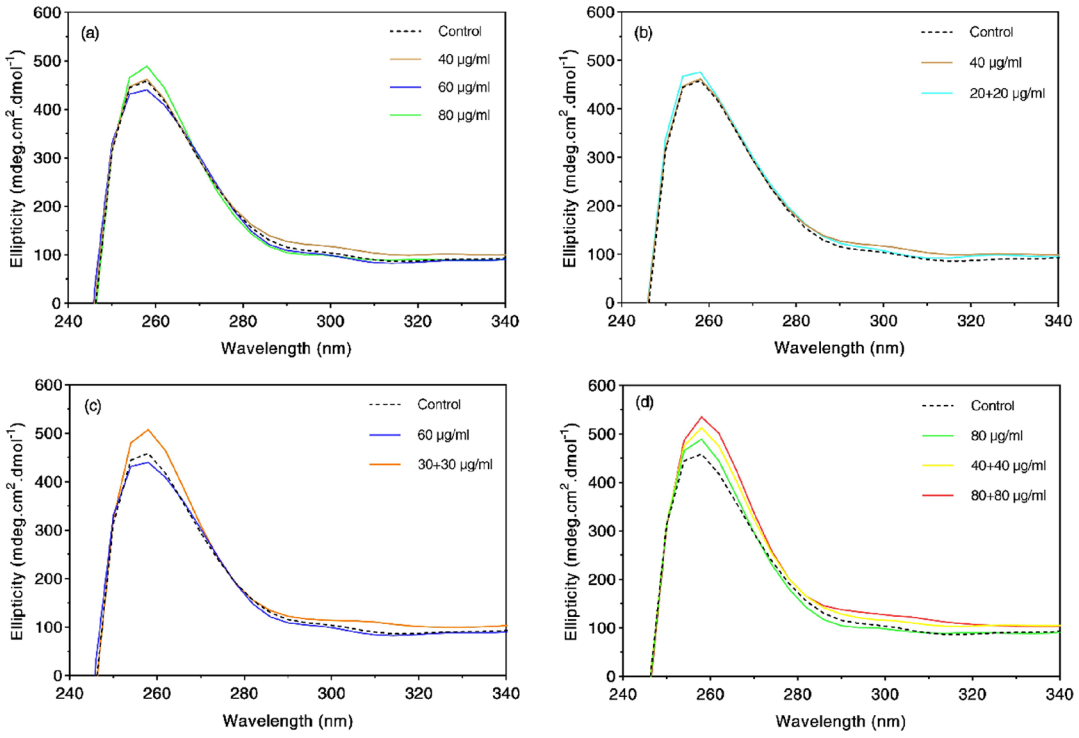

Figure 4. Near-UV spectral changes of ozonated and nonozonated Hb samples. (a) Near-UV spectra of control and 40, 60, and 80 μg/mL ozonated samples. (b) Near-UV spectra of control and 40 and 20 + 20 μg/mL ozonated samples. (c) Near-UV spectra of control and 60 and 30 + 30 μg/mL ozonated samples. (d) Near-UV spectra of control and 80, 40 + 40, and 80 + 80 μg/mL ozonated samples.

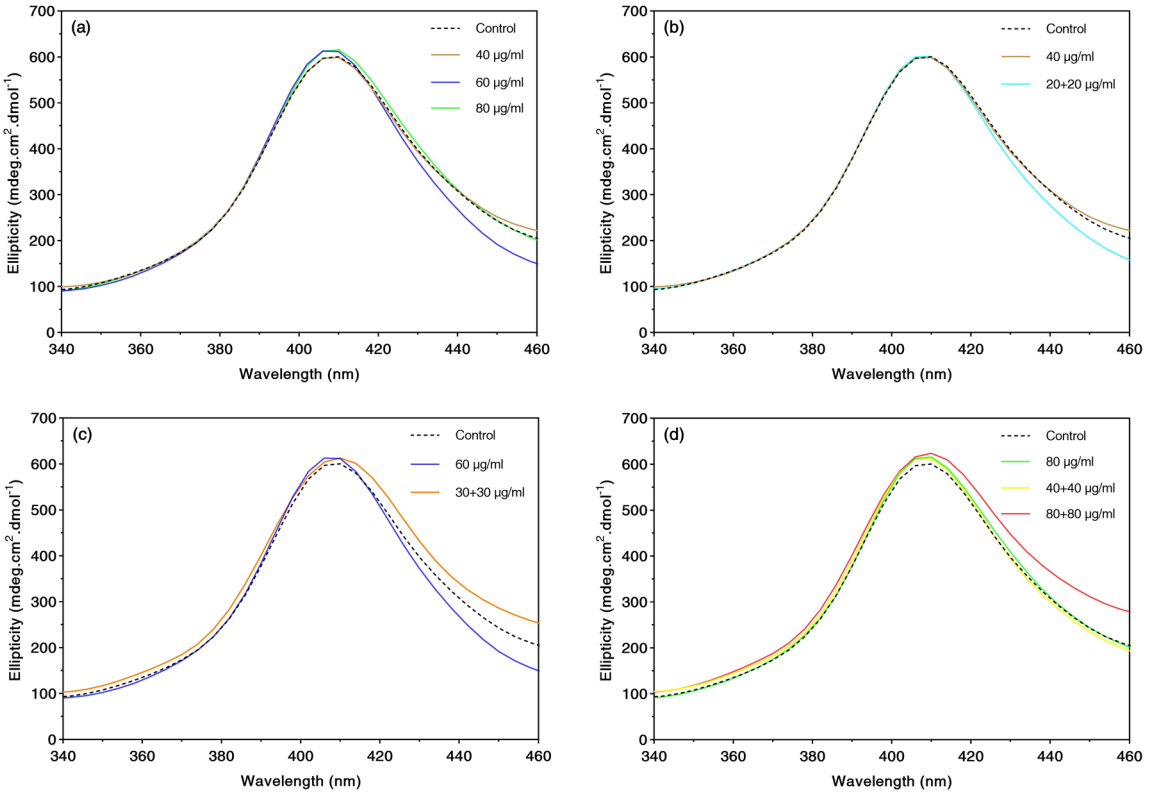

Figure 5. Soret-UV CD spectral changes of ozonated and nonozonated Hb samples. (a) Soret-UV spectra of control and 40, 60, and 80 μg/mL ozonated samples. (b) Soret-UV spectra of control and 40 and 20 + 20 μg/mL ozonated samples. (c) Soret-UV spectra of control and 60 and 30 + 30 μg/mL ozonated samples. (d) Soret-UV spectra of control and 80, 40 + 40, and 80 + 80 μg/mL ozonated samples.

fluorescence intensity for the 40, 60, and 80 μg/mL ozonated samples decreased only slightly compared to the control nonozonated sample (Figure 2a), indicating that perhaps the Trp, Tyr, and Phe residues are placed in a more exposed or

https://doi.org/10.1021/acsomega.3c01288
ACS Omega 2023, 8, 20714−20729

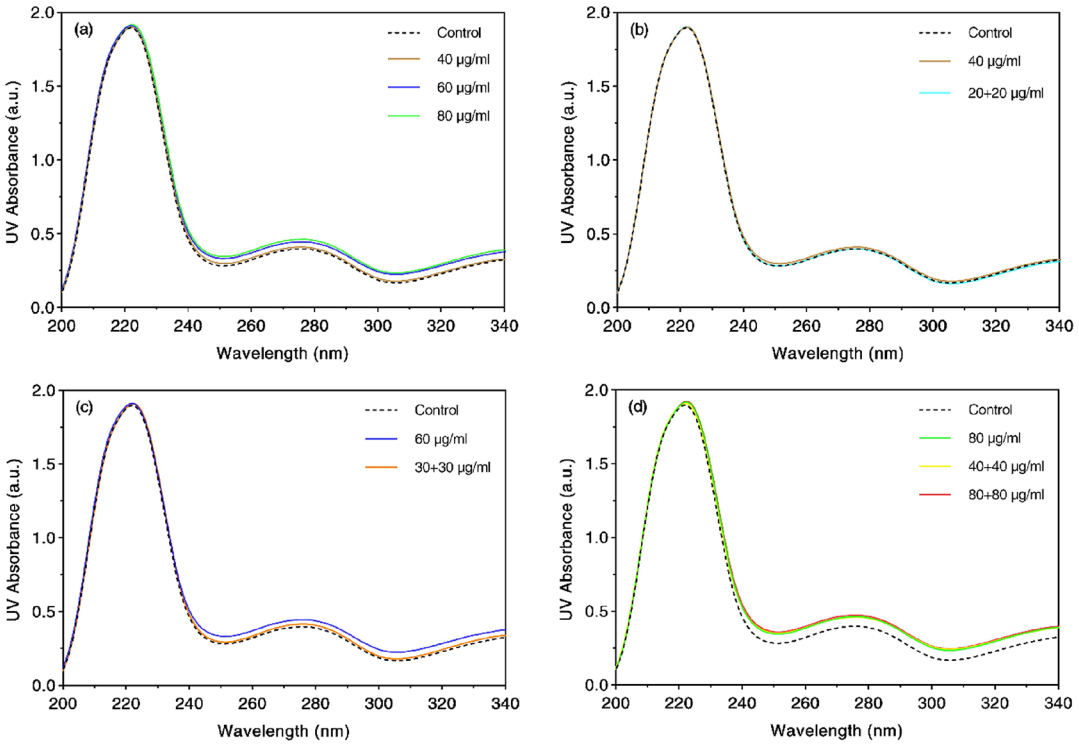

Figure 6. UV−vis absorption spectral changes of ozonated and nonozonated Hb samples in the wavelength range of 200 to 340 nm. (a) UV−vis absorption spectra of control and 40, 60, and 80 μg/mL ozonated samples. (b) UV−vis absorption spectra of control and 40 and 20 + 20 μg/mL ozonated samples. (c) UV−vis absorption spectra of control and 60 and 30 + 30 μg/mL ozonated samples. (d) UV−vis absorption spectra of control and 80, 40 + 40, and 80 + 80 μg/mL ozonated samples.

hydrophilic environment upon ozonation. No significant changes were seen when comparing the intrinsic fluorescence peak intensities of samples ozonated at 40, 60, and 80 μg/mL of ozone with the 20 + 20, 30 + 30, and 40 + 40 μg/mL ozonated samples, respectively (Figure 2b−d). As for the 80 + 80 μg/mL ozonated sample, the intrinsic fluorescence intensity was the lowest compared to the remaining ozonated samples (Figure 2d). Furthermore, in all ozonated samples, there was a slight shift toward longer wavelengths (red shift) relative to the control sample.

3.3. Circular Dichroism. *3.3.1. Far-UV Circular Dichroism.* Far-UV circular dichroism (CD) was used to investigate the secondary structural changes of Hb pre- and post-ozonation with different concentrations of ozone. In the far-UV CD spectrum of Hb, there are two negative absorption bands (minima) at 208 and 222 nm and a positive band at 193 nm, which are characteristics of the alpha-helical structure of proteins.[39] As seen in Figure 3a, the alpha-helical content of Hb slightly decreased as a function of ozone concentration, which may be due to alterations in the local environment of aromatic residues of the protein upon ozonation. In the case of 40 and 20 + 20 μg/mL ozonated samples (Figure 3b), the alpha-helical content of the protein of the 20 + 20 μg/mL sample was higher and was very similar to the control sample as opposed to the 40 μg/mL ozonated sample. No significant changes were seen when comparing the far-UV CD spectra of 60 and 80 μg/mL samples with the 30 + 30 and 40 + 40 μg/mL ozonated samples, respectively (Figure 3c,d). As for the 80 + 80 μg/mL ozonated sample, the alpha-helical content was the lowest compared to all the other ozonated samples (Figure 3d). Having said that, the shape and the peak position of the CD spectra for the ozonated samples did not change compared to the nonozonated sample, indicating that ozonation did not alter the overall secondary structure of Hb.

3.3.2. Near-UV CD. The CD spectrum in the near-UV region provides information on the arrangement of protein side-chain chromophore groups (aromatic residues) as well as changes in the disulfide bond, which reflects variations in the tertiary structure of the protein as a positive peak at 260 nm (L-band).[40] As shown in Figure 4a, the intensity of the 260 nm peak significantly increased for the 80 μg/mL ozonated sample compared to the control and 40 and 60 μg/mL ozonated samples, which may be attributed to an increase in the binding of heme to globin as a result of changes in the local environmental of aromatic residues. However, no significant changes were observed when comparing the L-band of the 40 μg/mL ozonated sample with the 20 + 20 μg/mL ozonated sample (Figure 4b). On the contrary, the L-band intensity for the 60 μg/mL sample was lower than that of the 30 + 30 μg/mL sample (Figure 4c), and similarly for the 80 μg/mL ozonated sample, the intensity was lower compared to the 40 + 40 μg/mL ozonated sample. As for the 80 + 80 μg/mL ozonated sample (Figure 4d), a significant increase in the intensity of L-band was seen compared to all other ozonated samples.

3.3.3. Soret-UV CD. The CD spectrum in the Soret-UV region shows changes in the heme group of Hb, including binding of the heme group to globin and oxygen, as a positive peak in the ∼414 nm region.[41] It can be seen from Figure 5a that there was a slight increase in the peak intensity of the 60 and 80 μg/mL ozonated samples compared to the control sample, whereas in the 20 + 20 and 40 μg/mL ozonated Hb samples, the peak intensities were similar to the control sample (Figure 5b). Additionally, the peak intensities of the 60 and 80 μg/mL ozonated samples were similar to the 30 + 30 and 40 + 40 μg/mL

https://doi.org/10.1021/acsomega.3c01288
ACS Omega 2023, 8, 20714−20729

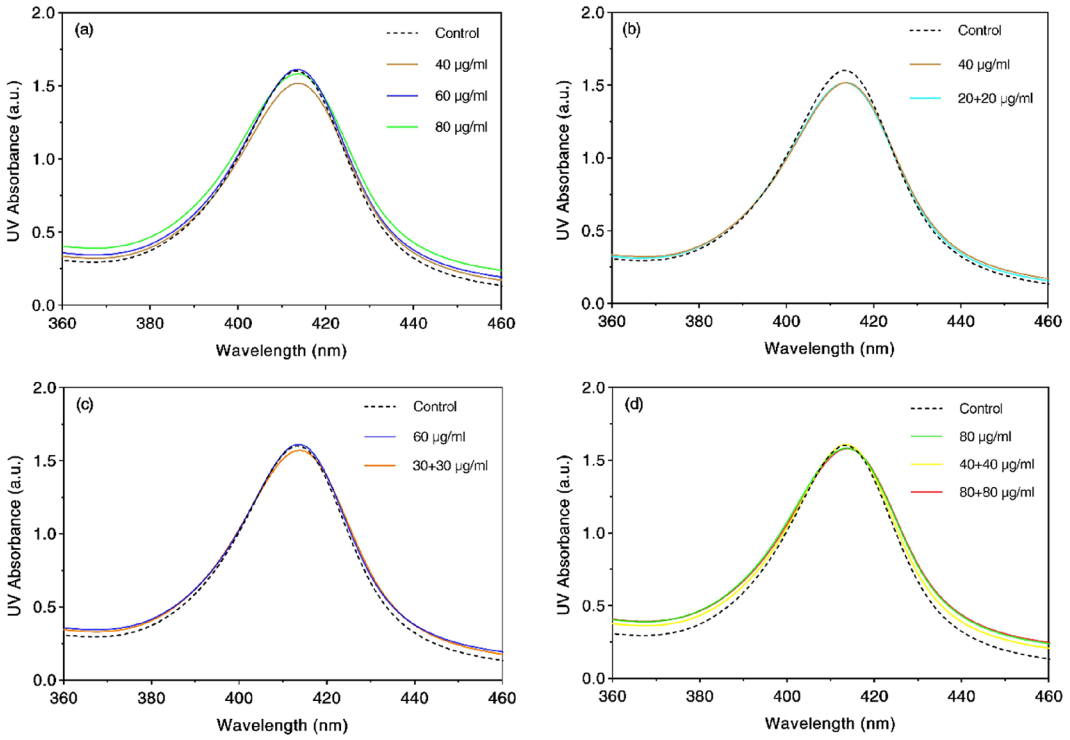

Figure 7. UV−vis absorption spectral changes related to 414 nm B- or Soret-band of ozonated and nonozonated Hb samples in the wavelength range of 360 to 460 nm. (a) UV−vis absorption spectra of control and 40, 60, and 80 μg/mL ozonated samples. (b) UV−vis absorption spectra of control and 40 and 20 + 20 μg/mL ozonated samples. (c) UV−vis absorption spectra of control and 60 and 30 + 30 μg/mL ozonated sample. (d) UV−vis absorption spectra of control and 80, 40 + 40, and 80 + 80 μg/mL ozonated samples.

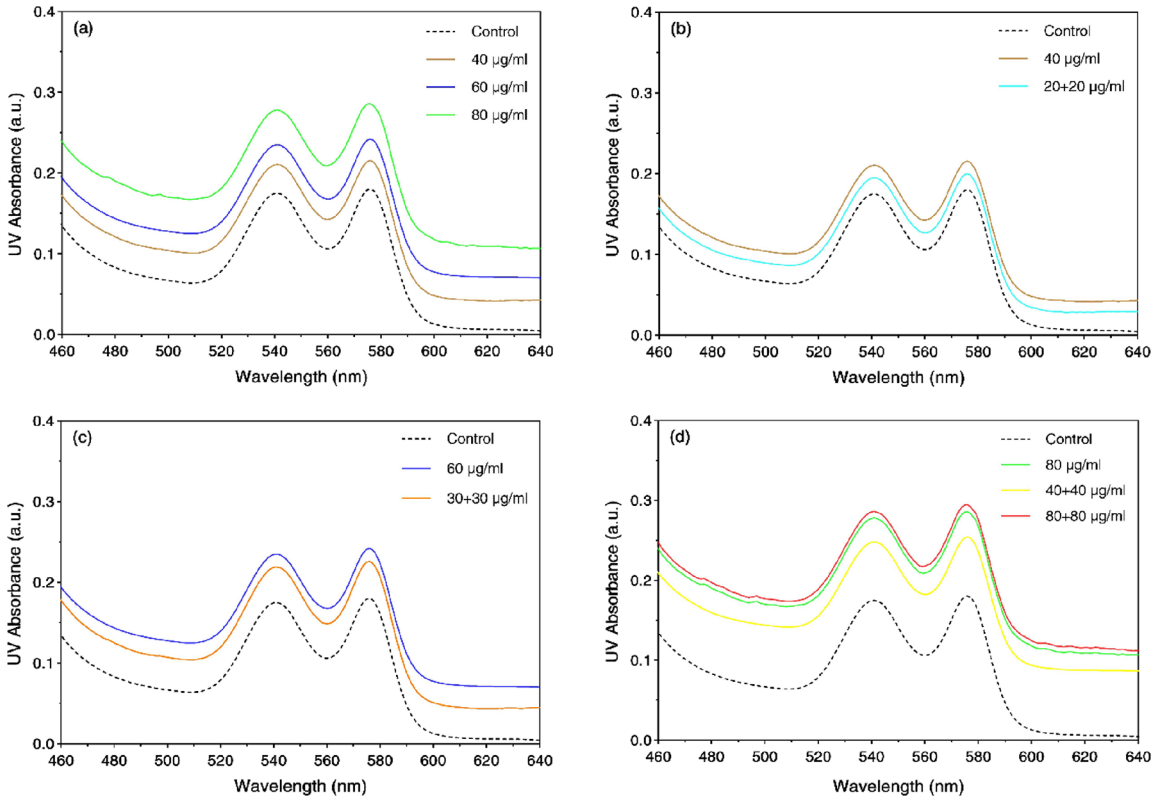

Figure 8. UV−vis absorption spectral changes of ozonated and nonozonated Hb samples related to 542 and 577 nm Q-bands in the wavelength range of 480 to 640 nm. (a) UV−vis absorption spectra of control and 40, 60, and 80 μg/mL ozonated samples. (b) UV−vis absorption spectra of control and 40 and 20 + 20 μg/mL ozonated samples. (c) UV−vis absorption spectra of control and 60 and 30 + 30 μg/mL ozonated samples. (d) UV−vis absorption spectra of control and 80, 40 + 40, and 80 + 80 μg/mL ozonated samples.

https://doi.org/10.1021/acsomega.3c01288
ACS Omega 2023, 8, 20714−20729

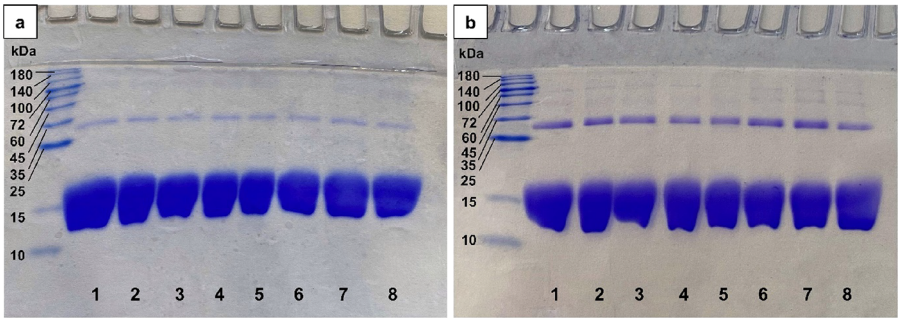

Figure 9. SDS-PAGE analysis of nonozonated and ozonated Hb samples in the presence of DTT (a) and absence of DTT (b). The order of the samples in the gels are as follows: first lane, protein marker; lanes 1−8, control (nonozonated) sample and ozonated samples at concentrations of 80 + 80, 20 + 20, 30 + 30, 40 + 40, 80, 60, and 40 μg/mL, respectively.

ozonated samples, respectively, and the highest Soret band intensity was related to the 80 + 80 μg/mL ozonated sample (Figure 5c,d).

3.4. UV−Vis Absorption Spectroscopy. UV−vis absorption spectroscopy is a powerful technique for analyzing secondary and tertiary structural changes of proteins as well as heme prosthetic group configuration and oxidation state in Hb.[42] UV−vis spectra of Hb in the range of 200−700 nm show a peak at 222 nm (peptide bond), 278 nm (aromatic residues), 414 nm (Soret-band), as well as 542 and 577 nm (Q-bands).[18,30] In all the samples studied, the intensity of the 222 nm bands overlapped greatly and did not change compared to the control nonozonated sample. Thus, increasing the ozone concentration did not lead to protein degradation. The changes related to aromatic residues at 278 nm also showed a slight increase for the 60 and 80 μg/mL samples as well as 40 + 40 and 80 + 80 μg/mL ozonated samples (Figure 6), which may be due to the oxidation of aromatic residues and alterations in their local microenvironment upon ozonation.

Changes related to binding of heme to globin can be deduced from the Soret-band intensity at 414 nm. As shown in Figure 7, there were no prominent changes in the intensity of the Soret-band with increasing ozone concentration.

However, in Figure 8, the intensity of the Q-bands was greater for the 40, 60, and 80 μg/mL ozonated samples compared to the 20 + 20, 30 + 30, and 40 + 40 ozonated samples, respectively, which indicated an increase in the binding of oxygen to the iron atom in the heme group. Out of the ozonated samples, the Hb sample ozonated at 80 + 80 μg/mL of ozone had the highest intensity peak.

3.5. SDS-PAGE Analysis. The SDS-PAGE results for the reduced and nonreduced Hb samples are shown in Figure 9. In both gels, either in the presence of dithiothreitol (DTT, a reducing agent) or in its absence (Figures 9a,b, respectively), there was a prominent band with a molecular weight of 15 kDa related to the monomeric Hb globins. A higher-molecular-weight band, between 25 and 35 kDa, was also observed in both gels, being more apparent under nonreducing conditions, which is plausible to be related to the Hb dimers formed as a result of dityrosine covalent cross-linkage upon ozonation.[43] In the absence of DTT, the dimeric globin bands varied in band intensity based on the single- or double-dose ozonation and also the concentration of ozone. As shown in Figure 9b, the dimeric band was more intense in lanes 2, 6, and 7, corresponding to 80 + 80, 80, and 60 μg/mL ozone. Furthermore, by increasing the ozone concentration and using single-dose instead of double-dose ozonation, additional bands with higher molecular weights were observed perhaps because of the formation of giant extracellular Hb[44] (Figure 9b). Hb oligomerization may have increased as a function of ozone concentration and single dose because of the oxidation of Tyr and Cys residues and the formation of covalent dityrosine cross-links and disulfide bonds. It appeared that ozonating twice, as observed in Figure 9b lanes 3−5, had the least amount of oligomerization.

3.6. Dynamic Light Scattering. Dynamic light scattering (DLS) is extensively used for obtaining data on the particle size distribution of macromolecules in solutions and for detecting protein oligomers.[45] The DLS results for the nonozonated and ozonated Hb samples in both number and intensity modes are given in Table 3, and the size distribution of Hb samples revealed by DLS in the number mode is shown in Figure 10. The particle size distribution in the number mode showed that the control nonozonated Hb sample had an estimated diameter size of 5.1 nm. However, upon ozonation, the diameter size increased gradually in an ozone-concentration-dependent

Table 3. Zeta Potential Values and Diameter Size of Nonozonated and Ozonated Hb Samples in Number and Intensity Modes[a]

samples	zeta potential (mV)	diameter (nm) (number mode)	diameter (nm) (intensity mode)	intensity (%) (intensity mode)
control	−18.7	5.1	11.0	69
			706.9	31
20 + 20 μg/mL	−13.3	7.3	9.3	11
			1108	89
40 μg/mL	−9.9	7.9	8.9	5
			1411.6	95
30 + 30 μg/mL	−8.5	8.2	10.1	8
			1023.1	92
60 μg/mL	−7.2	15.1	17.1	8
			1132.3	92
40 + 40 μg/mL	−6.0	23.3	39.3	16
			1491.8	84
80 μg/mL	−5.4	33.6	34.5	11
			775.6	89
80 + 80 μg/mL	−2.2	68.0	73.2	29
			623.1	71

[a]The first column shows the sample type description; the second column indicates the zeta potential values in millivolts; the third and fourth columns provide the diameter size in number and intensity modes, respectively; and the fifth column indicates the percentage intensity values.

https://doi.org/10.1021/acsomega.3c01288
ACS Omega 2023, 8, 20714−20729

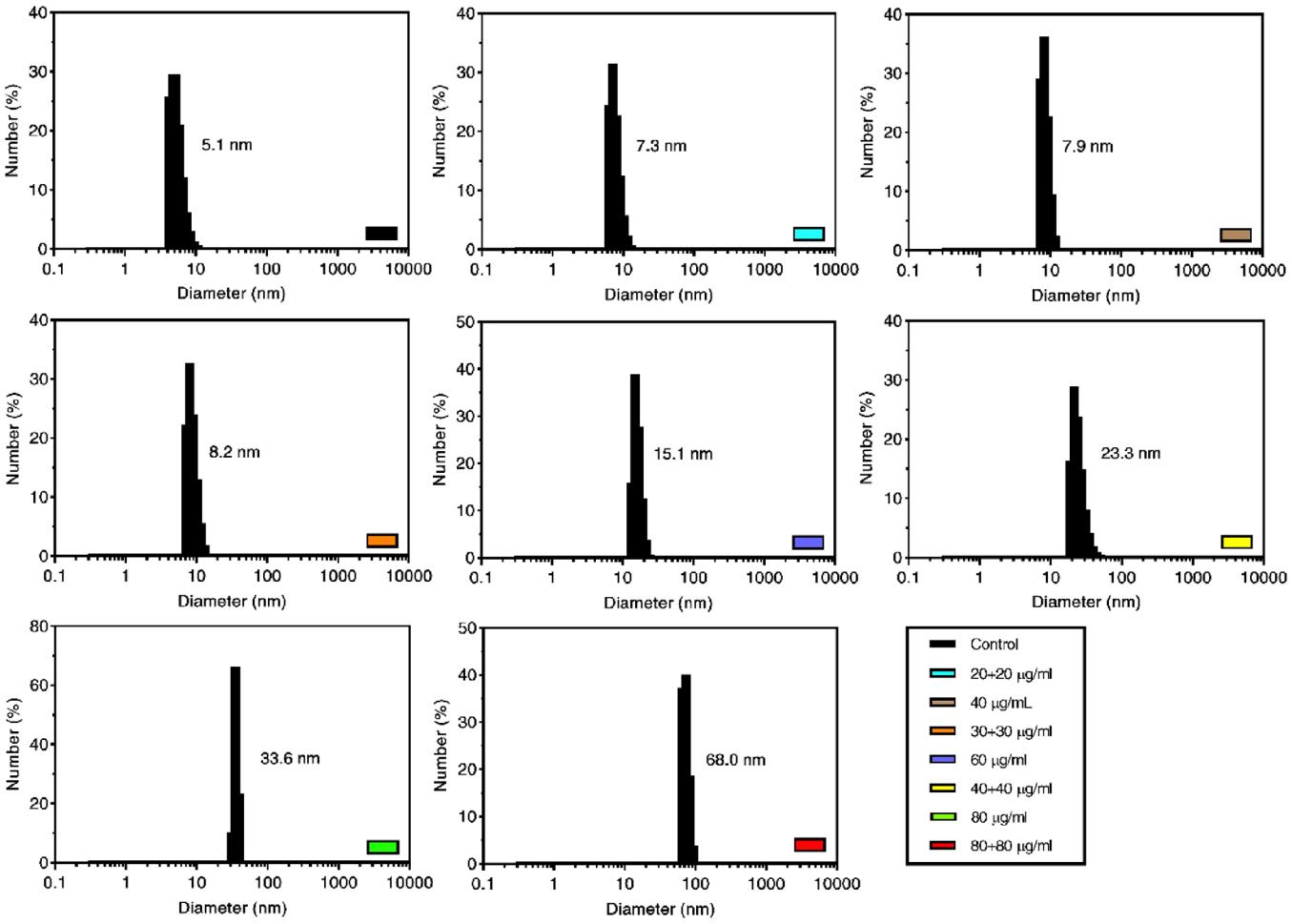

Figure 10. DLS profiles of nonozonated and ozonated Hb samples. The peak diameter values in number mode are expressed in nanometers. For intensity mode values and intensity percentage, please refer to Table 3.

manner. The particle size distribution in terms of the intensity mode also increased as a function of ozone concentration because of the formation of oligomeric species, which was also evident in the SDS-PAGE results. In addition, the oligomer diameter sizes in the 40, 60, and 80 μg/mL ozonated samples were larger than those in the 20 + 20, 30 + 30, and 40 + 40 μg/mL samples, respectively. Therefore, it can be concluded that using ozone concentrations of 20 + 20, 30 + 30, and 40 + 40 μg/mL instead of 40, 60, and 80 μg/mL can reduce the adverse effects of ozonation on Hb oligomerization. In the case of Hb samples ozonated with 80 + 80 μg/mL of ozone, the diameter size as well as the number of oligomeric species increased significantly compared to the other ozone-treated samples.

3.7. Zeta Potential. The zeta potential is a parameter for determining the magnitude of surface charge distribution corresponding to attraction/repulsion between particles and can provide information on particle size stability.[46] The zeta potential results of nonozonated and ozonated Hb samples are given in Table 3 as well as Figure 11. The control nonozonated sample has an estimated zeta potential value of −18.7 mV; however, this value decreased gradually as a function of ozone concentration. As for the 80 + 80 μg/mL ozonated sample, the zeta potential value decreased to −2.2 mV, which signified greater instability of the protein. The decrease in zeta potential value with increasing ozone concentration may be due to the reduction of electrostatic repulsion forces and accumulation of

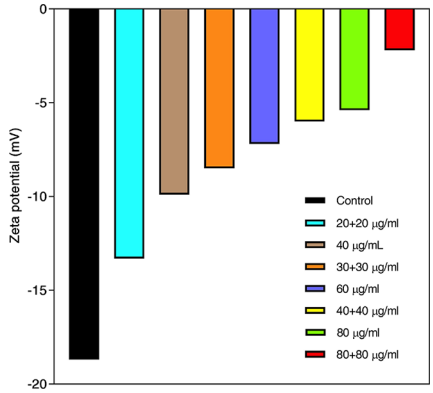

Figure 11. Zeta potential measurements of nonozonated and ozonated Hb samples, expressed in millivolts. The zeta potential values indicate the surface charge on Hb. For more information on the zeta potential values, please refer to Table 3.

Hb particles. Furthermore, the zeta potential values of the 40, 60, and 80 μg/mL ozonated samples were lower than those of the 20 + 20, 30 + 30, and 40 + 40 μg/mL ozonated samples, respectively.

3.8. Sequence and Structural Analyses of Hb Autoxidation Sites. *3.8.1. Residues Involved in the Autoxidation of Hb.* Previously, the sequences and structures of Hb from two species of Caspian Sea sturgeon, *Acipenser stellatus* (PDB ID

https://doi.org/10.1021/acsomega.3c01288
ACS Omega 2023, 8, 20714−20729

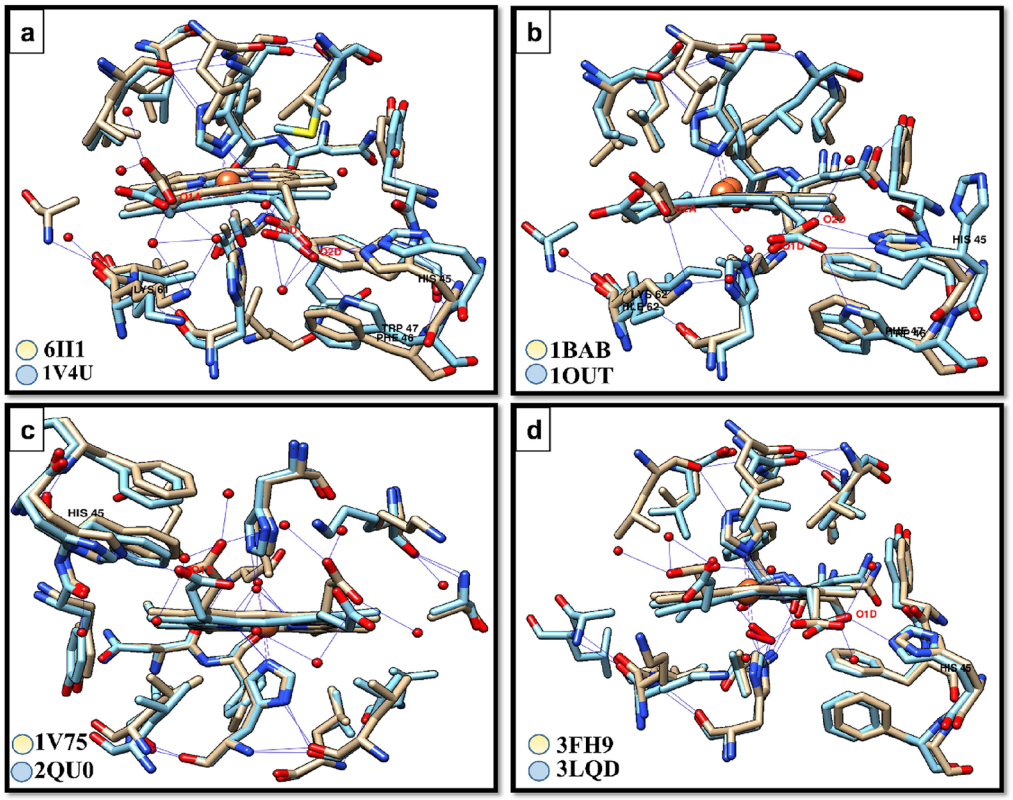

Figure 12. Structural analysis of alpha globin prosthetic groups in the (a) CO-Hb, (b) deoxy-Hb, (c) Met-Hb, and (d) Oxy-Hb states. Gold and blue colors correspond to PDB IDs with the highest and lowest number of water molecules in the heme pocket, respectively. The heme pocket residues are shown in sticks and labeled with three-letter abbreviations; the propionate group oxygens are labeled as O1A, O2A, O1D, and O2D; water molecules are shown as small red spheres; hydrogen bonds are shown as lines; and covalent bonds are shown as broadened lines. Figures were generated using Chimera.

6IYI) and *Acipenser persicus* (PDB ID 6IYH), were identified, and it was found that the former structure had five water molecules and the latter had four water molecules inside their heme pocket of the alpha globin.[21] In the present study, a protein BLAST search was done using the PDB ID: 6IYI as a reference protein structure with a relatively high number of water molecules, and a total of 100 structures were obtained for both alpha and beta globins (Figure S1), out of which 63 structures were selected for the alpha globin and 47 structures were selected for the beta globin after omitting the mutated and complexed forms of the Hb proteins. Then, using LigPlot,[35] the residues involved in the Hb heme autoxidation as well as their interactions with the heme prosthetic group were analyzed. The Chimera visualization and analysis tool[34] was used to determine the number of water molecules present in the heme pocket as well as the type of interaction and distance between the heme group and nearby residues. The results for all the selected Hbs are displayed in Tables S1 and S2 for alpha and beta globins, respectively.

It was found that, in the alpha and beta globins, the Trp, Tyr, and Phe residues were in contact with the heme group through hydrogen bonding and hydrophobic interactions and that the heme prosthetic group was located in a hydrophobic pocket. Particularly in alpha globin, hydrophobic residues including Tyr42, Phe43, Phe46, histidine (His)58, lysine (Lys)61, Val62, leucine (Leu)83, Leu86, Leu91, Val93, asparagine (Asn)97, Phe98, Leu101, and Leu136 were present near the Hb heme group, whereas in beta globin, threonine (Thr)38, Phe41, Phe42, His63, Lys66, Val67, serine (Ser)70, Leu88, Leu91, Leu96, Val98, Asn102, Phe103, Leu106, and Leu141 were found near the Hb heme group. Furthermore, in addition to Met-Hb, there were a number of water molecules within the heme pocket in CO-Hb, deoxy-Hb, and Oxy-Hb states in both alpha and beta globins.

3.8.2. Number of Water Molecules in the Hb Heme Pocket. In the next step, initially the structures of alpha globins that had the highest and lowest number of water molecules in their heme pocket, for all the heme states including CO, deoxy, Met, and Oxy states, were compared (Tables S3−S7). For the deoxy-Hb state of alpha globins, there were two structures with the highest number of water molecules in their heme pocket, and therefore, the two structures were analyzed separately in Tables S4 and S5. Additionally, the results from comparing beta globins that had the highest and lowest number of water molecules in their heme pocket, in all heme states, were compared (Tables S8−S12). Similar to the alpha globin analysis, the deoxy state of beta globins had two structures with highest number of water molecules in their heme pocket, and hence, the two structures were analyzed separately in Tables S9 and S10. On the basis of the results obtained from Tables S3−S12, it was found that the presence or displacement of certain amino acids in the alpha and beta globins in all heme states led to the entry of water molecules into the heme pocket. Phe46 and Lys61 in the CO and deoxy states, and His45 in the Met state of alpha globin, allowed more water molecules to enter the heme moiety. Thr66 and Ile96 in the CO state and Val66, Thr91, and Met141 in the deoxy state of beta globin, allowed more water molecules to enter the heme pocket.

https://doi.org/10.1021/acsomega.3c01288
ACS Omega 2023, 8, 20714−20729

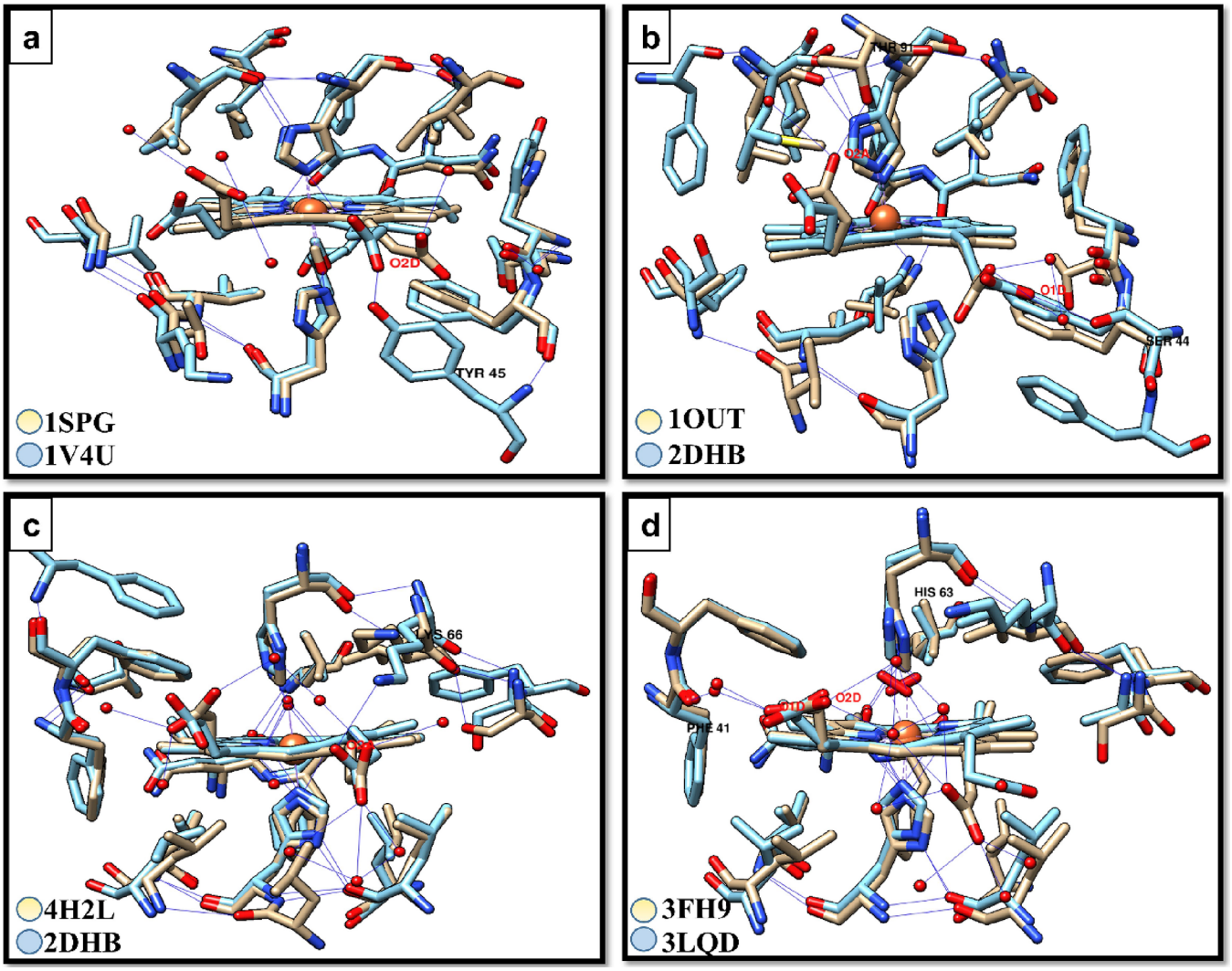

Figure 13. Structural analysis of beta globin prosthetic groups in the (a) CO-Hb, (b) deoxy-Hb, (c) Met-Hb, and (d) Oxy-Hb states. Gold and blue colors correspond to PDB IDs with the highest and lowest water molecules in the heme pocket, respectively. The heme pocket residues are shown in sticks and labeled with three-letter abbreviations; the propionate group oxygens are labeled as O1A, O2A, O1D, and O2D; water molecules are shown as small red spheres; hydrogen bonds are shown as lines; and covalent bonds are shown as broadened lines. Figures were generated using Chimera.

3.8.3. Structural Analysis of the Heme Propionate Groups. To determine which residues had a more significant role in increasing the number of water molecules in the heme pocket, the prosthetic groups of structures with the highest number of water molecules and those that had the lowest number of water molecules were compared separately for each Hb state. For the alpha globin, in the CO-Hb state, two structures with PDB IDs 6II1 (H_2O n = 7) and 1V4U (H_2O n = 0) were compared (Figure 12a). Structural analysis of propionate groups of these two structures showed that Lys61 in the 6II1 structure was associated with the propionate group of heme through a hydrogen bond with O1A, whereas in the 1V4U structure, there was no interaction with the propionate group. Also, His45 was associated with the propionate group of heme via a hydrogen bond with O1D in the 6II1 structure, whereas in 1V4U, His45 was bound to O2D via hydrogen bonding. In the 1V4U structure, Trp47 (which was actually located in position 46) was associated with the propionate group via hydrogen bonding with O2D, whereas in the 6II1 structure, this position was occupied by Phe46, and there were no interactions with propionate group oxygens. For the deoxy-Hb state, two PDB structures, 1BAB (H_2O n = 3) and 1OUT (H_2O n = 0), were compared (Figure 12b). Structural analysis of the propionate groups of these two structures showed that Lys62 in 1BAB (which was actually located in position 61) was associated with the O2A of the propionate group through hydrogen bonding. Lys62 was also associated with a water molecule through hydrogen bonding, and the water molecule was hydrogen bonded to the O1D of the propionate group and the distal histidine. On the other hand, in the 1OUT structure, Ile62 (which was actually located in position 61) had no association with the propionate group oxygens. However, His45 hydrogen bonded to the O2D of the propionate group in both structures. In the 1OUT structure, Trp46 established a hydrogen bond with O2D of the propionate group, whereas in the 1BAB structure, the same position was occupied by Phe47 (which was actually located at position 46), and there were no interactions with the propionate group oxygens. For the Met-Hb state, two structures, 1V75 (H_2O n = 8) and 2QU0 (H_2O n = 0), were compared (Figure 12c). Structural analysis of the propionate groups of these two structures showed that His45 in the 1V75 structure formed a hydrogen bond with O1D of the propionate group; as for the

https://doi.org/10.1021/acsomega.3c01288
ACS Omega 2023, 8, 20714−20729

2QU0 structure, there was no association with the propionate group. For the Oxy-Hb state, two structures with PDB IDs 3FH9 (H_2O n = 6) and 3LQD (H_2O n = 0) were compared (Figure 12d). The structural analysis of the propionate groups of these two structures showed that His45 in the 3LQD structure formed a hydrogen bond with O1D of the propionate group, whereas in the 3FH9 structure, there were no interactions with the propionate group oxygens.

As for the beta globins, in the CO-Hb state, two structures, 1SPG (H_2O n = 4) and 1V4U (H_2O n = 0), were compared (Figure 13a). The structural analysis of the propionate groups of these two structures showed that in the 1V4U structure, Tyr45 was hydrogen bonded to the O2D of the propionate group, whereas in 1SPG, Phe45 had no interaction with the propionate group oxygens. For the deoxy-Hb state, two structures, 1OUT (H_2O n = 3) and 2DHB (H_2O n = 0), were compared (Figure 13b). The structural analysis of the propionate groups of these structures showed that in 2DHB, Ser44 was hydrogen bonded to the O1D of the propionate group, whereas in 1OUT, Ser44 had no interaction with the propionate group oxygens. However, in the 1OUT structure, the Thr91 residue was hydrogen bonded to O2A of the propionate group, whereas in the 2DHB structure, a Leu occupied this position, which had no interaction with the propionate group oxygens. As for the Met-Hb state, two structures, 4H2l (H_2O n = 8) and 2ZFB (H_2O n = 0), were compared (Figure 13c). The structural analysis of the propionate groups of these two structures showed that Lys66 in the 2ZFB structure formed a hydrogen bond with O2A oxygen of the propionate group, whereas in the 4H2I structure, there was no interaction with the propionate group oxygens. For the Oxy-Hb state, two structures, 3FH9 (H_2O n = 9) and 3LQD (H_2O n = 0), were compared (Figure 13d). The structural analysis of the propionate groups of these two structures showed that in the 3FH9 structure, Phe41 hydrogen bonded to a water molecule, and the water molecule was hydrogen bonded to the O1D of the propionate group. His63 was also hydrogen bonded to a water molecule, and this water molecule was hydrogen bonded to the O2D of the propionate group in the 3FH9 structure.

3.8.4. Sequence Comparison Between Alpha and Beta Globins and the Structural Flexibilty of Propionate Groups. Sequence analysis of alpha globins with the highest number of water molecules in the heme pocket and of alpha globins with the least number of water molecules in each of the CO, deoxy, Met, and Oxy states are shown in Figures S2−S5, respectively. The results for the CO, deoxy, Met, and Oxy states of beta globin are shown in Figures S6−S9. On the basis of the results obtained from Figures S2−S5, it was found that, in the alpha globin, the sequence identity percentage for the CO state Hbs across 137 residues varied from 47 to 87%. Additionally, the sequence identity percentage in the deoxy state Hbs across 141 residues varied from 57 to 87%. In the case of Met-Hbs, the sequence identity percentage of alpha globins varied from 48 to 57% across 141 residues. It should be noted that in the case of Oxy-Hbs, the sequence identity percentage of alpha globins across 141 residues varied from 66 to 82%.

On the basis of the results obtained from Figures S6−S9, it was found that, in the beta globins, the sequence identity percentage for the CO state Hbs varied between 50 and 64% across 145 residues. Also, the sequence identity in the deoxy state of beta globins varied between 45 and 99% across 146 residues. In the Met state, the sequence identity percentage varied between 66 and 97% across 146 residues. In the Oxy state, the sequence identity percentage across 146 residues varied between 51 and 91%.

It was also found that the sequence identity percentage in the beta globin was higher than that in the alpha globin, indicating the higher structural diversity in the alpha globin. Furthermore, the heme propionate groups in the alpha and beta globins, in all heme states, had different orientations, especially in the deoxy state.

4. DISCUSSION

Herein, the effects of different concentrations of ozone on human Hb were investigated through molecular and spectroscopic analytical techniques with an emphasis on the single- versus double-dose-dependent action of ozone on Hb. The VBG analysis of whole blood ozonated samples indicated that the pH, partial pressure, and saturation percentage of oxygen upon ozonation differ from the nontreated whole blood sample. Increasing the ozone concentration led to a decrease in pH and increased the PO_2 and saO_2 levels. Intrinsic fluorescence spectra of the purified Hb samples at λ_{ex} = 280 nm showed a slight decrease in the intrinsic fluorescence peaks of the ozonated samples compared to the nonozonated sample, which indicates that the local environment of the Hb fluorophores was slightly changed postozonation. However, the presence of antioxidants in the whole blood prevented major alterations upon treatment with ozone.[18] Additionally, the far-UV CD analysis showed that the alpha helical content of the ozonated samples decreased relative to the nonozonated sample, whereas the overall secondary structure of Hb was not altered upon ozonation. As for the near-UV CD, no major changes were seen in the ozonated samples compared to the control Hb sample. Detailed analysis of purified nonozonated and ozonated Hb samples using techniques such as UV−vis spectroscopy did not show major signs of Hb degradation upon ozonation as there were only slight changes in the peptide bond, aromatic residues, and Soret-band peaks. On the contrary, the peak intensities for the Q-bands increased as the ozone concentration increased, which was a sign of enhanced oxygen binding affinity to Hb. Moreover, the peak intensities were higher for the 40, 60, and 80 μg/mL ozonated samples compared to the 20 + 20, 30 + 30, and 40 + 40 μg/mL ozonated samples, respectively. Furthermore, all the Hb ozonated samples were in the Oxy state and no Met-Hb were detected, similar to the findings in previous studies.[30] All of the aforementioned techniques were found to be useful for determining the effect of ozone on Hb; however, SDS-PAGE, DLS, as well as zeta potential were found to be the most appropriate for deducing the overall effects of ozonation on Hb. The DLS results indicated the formation of higher-molecular-weight Hb oligomers especially for higher ozone concentrations, as seen by diameter size changes in the Hb tetramer from ∼5 nm[47] to larger values, which were also consistent with the SDS-PAGE results and in line with previous studies.[18,30,43] As for the zeta potential measurements, the stability of Hb decreased with increasing ozone concentration shown as smaller negative zeta potential values. Interestingly, the changes in zeta potential values as well as SDS-PAGE and DLS were less when two doses of ozone were used instead of a single dose of ozone. Moreover, ozonating whole blood with 80 + 80 μg/mL of ozone did not show major harmful effects on Hb, which is partly due to the presence of antioxidants in the blood that make Hb less prone to structural changes.[5] However, SDS-PAGE, DLS, and zeta potential results showed a noticeable increase in the formation of oligomeric species and instability of the Hb in the 80 + 80 μg/

https://doi.org/10.1021/acsomega.3c01288
ACS Omega 2023, 8, 20714−20729

mL ozonated samples. Additionally, a previous study has shown that increasing ozone concentration to 160 μg/mL through *in vitro* MAH induces hemolysis and morphological changes of erythrocytes in both aortic dissection (AD) patients and healthy individuals.[6] Hence, the changes in the Hb treated with 80 + 80 μg/mL of ozone may be attributed to the overdosed ozone concentration.

In the second part of this study, the residues involved in autoxidation of Hb were analyzed using sequence and structural analysis tools. Through detection of changes observed in the heme propionate groups for all the Hb states, different orientations were observed in alpha and beta globins, which may be due to different local heme environments. It is worth mentioning that structural diversity of propionate groups in all heme states was more prominent in the alpha globin than the beta globin, which is in agreement with previous reports.[21] Furthermore, the results showed that there were a large number of water molecules inside the heme pocket in both alpha and beta globins for all heme states. However, this number was higher in the alpha globin compared to the beta globin. Hence, it can be concluded that the autoxidation rate in the alpha globin is higher, as seen in previous studies.[21,25]

In the first part of this study, it was shown that ozone effects Trp, Tyr, and Phe residues. As for the second part of this study, it was shown that the aforementioned residues were associated with the heme propionate groups of Hb through hydrogen bonding and hydrophobic interactions and that the presence of aromatic residues such as Phe enhances Hb autoxidation. Indeed, the results showed that in the CO and deoxy states of alpha globin, Phe46 and Lys61 and, in the Met state, His45 led to structural changes by changing the orientation of the propionate groups and therefore allowing more water molecules to enter the heme moiety. Additionally, structural analysis of the beta globins revealed that the presence of Thr66 and Ile96 in the CO state of beta globin and Val66, Thr91, and Met141 in the deoxy state of beta globin allowed more water molecules to enter the heme pocket and thus resulted in the increase of heme autoxidation rate. In the deoxy state of the beta globin, Thr91 and, in the Oxy state, Phe41 and His63 changed the orientation of the propionate groups and as a result increased the number of water molecules in the heme pocket. In fact, the presence and displacement of certain amino acids around the Hb heme lead to the entry of water molecules into the heme pocket, which plays an important role in creating oxidative stress and ultimately causing Hb autoxidation.

5. CONCLUSIONS

The present study confirms that a single dose and double dose of ozonation, with the same total concentration, have varying effects on Hb. This was verified by results from ozonating whole blood samples with double doses of 20, 30, and 40 μg/mL ozone versus ozonating them with a single dose of 40, 60, and 80 μg/mL ozone, which showed that the former ozonation method leads to decreased unfavorable effects in the Hb structure. Two of the methods used in this study including DLS and SDS-PAGE indicated the formation of more oligomeric Hb particles, especially when single doses of high ozone concentrations were used. The stability of Hb also decreased as a function of ozone concentration, as seen by the decrease in negative zeta potential values, which was more prominent in the single-dose ozonated samples compared to double-dose ozonated Hb samples. Taken together, the findings of this study imply that the suitable and personalized ozone concentration for the participant who donated blood in the present study was 40 μg/mL because no significant changes were observed in the 40 μg/mL treated Hb sample compared to the nonozonated control sample. Additionally, it was apparent that using double doses of 20 μg/mL was even better than using a single dose of 40 μg/mL of ozone for the participant who donated blood in this study, showing that unfavorable effects could be eliminated by a two-dose versus one-dose ozone mixture with blood. Hence, it can be suggested that when a certain dose of ozone in MAH is selected without enough tests, then a double-dose method would better favor the patient and avoid unnecessary complications, especially when the blood antioxidant levels vary from one patient to another. It should be noted that these findings cannot be extrapolated to all patients and the appropriate ozone dosage should be assessed for each individual prior to MAH. Moreover, SDS-PAGE, DLS, and zeta potential results showed an increase in the diameter size and instability of the Hb samples for the samples treated with 80 + 80 μg/mL of ozone. As for the second part of this study, it was found that the autoxidation rate in the alpha globin is higher than that in the beta globin. The presence of Lys61 and Phe46 in both the CO-Hb and deoxy-Hb states and His45 in the Met-Hb state of alpha globins and also the existence of Thr66 and Ile96 in the CO-Hb state; Val66, Thr91, and Met141 in the deoxy-Hb state; and Phe41and His63 in the Oxy-Hb state of beta globins allow entry of water molecules into the heme pocket, which can eventually lead to heme autoxidation.

■ ASSOCIATED CONTENT

Supporting Information

The Supporting Information is available free of charge at https://pubs.acs.org/doi/10.1021/acsomega.3c01288.

Analysis of binding interactions between residues, ligands, and water molecules with the heme prosthetic group of the alpha and beta globin of Hb (Tables S1 and S2); binding interactions of different residues with the heme prosthetic group of alpha globins (Tables S3−S7) and beta globins (Tables S8−S12); multiple sequence alignment of alpha and beta globin sequences of all the analyzed Hbs (Figure S1); and structural and sequence comparison of alpha globins (Figures S2−S5) and beta globins (Figure S6−S9) (PDF)

■ AUTHOR INFORMATION

Corresponding Author

Arefeh Seyedarabi − *Department of Biochemistry, Institute of Biochemistry and Biophysics, University of Tehran, Tehran 1417614411, Iran;* orcid.org/0000-0003-4234-9799; Phone: +(98) 21-66956974; Email: a.seyedarabi@ut.ac.ir

Authors

Ramin Naderi Beni − *Department of Biochemistry, Institute of Biochemistry and Biophysics, University of Tehran, Tehran 1417614411, Iran*

Zahra Hassani-Nejad Pirkouhi − *Department of Biochemistry, Institute of Biochemistry and Biophysics, University of Tehran, Tehran 1417614411, Iran*

Fouad Mehraban − *Department of Biochemistry, Institute of Biochemistry and Biophysics, University of Tehran, Tehran 1417614411, Iran*

Complete contact information is available at: https://pubs.acs.org/10.1021/acsomega.3c01288

Author Contributions

R.N.B.: Sample collection, methodology, data investigation, formal analysis, writing and preparing the original draft. Z.H.P.: Methodology, data investigation, writing and preparing the original draft. F.M.: Assistance in analyzing data, reviewed and edited the final version of the manuscript. A.S.: Methodology, data investigation, conceptualized the research topic, acquired funds, supervision, reviewed and edited the final version of the manuscript. All authors read and approved the final manuscript.

Funding

The present study was funded by the Research Council of University of Tehran.

Notes

The authors declare no competing financial interest.

This study was reviewed and approved by the Ethics Committee of the School of Science, University of Tehran (IR.UT.SCIENCE.REC.1400.010).

■ ACKNOWLEDGMENTS

We thank Mr. Vahid Mirzaaghaei, the founder of Gardina Corporation and manufacturer of ozone therapy medical devices in Iran, for providing the Gardina ozone generator for medical use in the present study. We also thank Ms. Maryam Fahimifar from the ozone therapy clinic in Tehran, Iran, for her assistance in blood collection and *ex vivo* ozonation and the Tehran Heart Center staff for VBG analysis.

■ ABBREVIATIONS

MAH: major autohemotherapy
Hb: hemoglobin
Nrf2: nuclear factor erythroid 2-related factor 2
VBG: venous blood gas
CD: circular dichroism
SDS-PAGE: SDS-polyacrylamide gel electrophoresis
DTT: dithiothreitol
DLS: dynamic light scattering

■ REFERENCES

(1) Elvis, A. M.; Ekta, J. S. Ozone Therapy: A Clinical Review. *J. Nat. Sci. Biol. Med.* **2011**, *2*, 66−70.
(2) Bocci, V. *Ozone A New Medical Drug*; Springer, 2005. https://doi.org/10.1007/1-4020-3140-8.
(3) Bocci, V. A.; Zanardi, I.; Travagli, V. Ozone Acting on Human Blood Yields a Hormetic Dose-Response Relationship. *J. Transl. Med.* **2011**, *9*, 66.
(4) Schwartz-Tapia, A.; Martínez-Sánchez, G.; Sabah, F.; Alvarado-Guémez, F.; Bazzano-Mastrelli, N.; Bikina, O.; Borroto-Rodrígez, V.; Cakir, R.; Clavo, B.; González-Sánchez, E. Madrid Declaration on Ozone Therapy. *ISCO3: Madrid, Spain* 2015, *50*.
(5) Travagli, V.; Zanardi, I.; Silvietti, A.; Bocci, V. A Physicochemical Investigation on the Effects of Ozone on Blood. *Int. J. Biol. Macromol.* **2007**, *41*, 504−511.
(6) Deng, L.; Meng, W.; Li, D.; Qiu, D.; Wang, S.; Liu, H. The Effect of Ozone on Hypoxia, Hemolysis and Morphological Change of Blood from Patients with Aortic Dissection (AD): A Preliminary in Vitro Experiment of Ozonated Autohemotherapy for Treating AD. *Am. J. Transl. Res.* **2018**, *10*, 1829−1840.
(7) Sagai, M.; Bocci, V. Mechanisms of Action Involved in Ozone Therapy: Is Healing Induced via a Mild Oxidative Stress? *Med. Gas Res.* **2011**, *1*, 29.
(8) Clavo, B.; Martínez-Sánchez, G.; Rodríguez-Esparragón, F.; Rodríguez-Abreu, D.; Galván, S.; Aguiar-Bujanda, D.; Díaz-Garrido, J. A.; Cañas, S.; Torres-Mata, L. B.; Fabelo, H.; Téllez, T.; Santana-Rodríguez, N.; Fernández-Pérez, L.; Marrero-Callico, G. Modulation by Ozone Therapy of Oxidative Stress in Chemotherapy-Induced Peripheral Neuropathy: The Background for a Randomized Clinical Trial. *Int. J. Mol. Sci.* **2021**, *22*, 2802.
(9) Pecorelli, A.; Bocci, V.; Acquaviva, A.; Belmonte, G.; Gardi, C.; Virgili, F.; Ciccoli, L.; Valacchi, G. NRF2 Activation Is Involved in Ozonated Human Serum Upregulation of HO-1 in Endothelial Cells. *Toxicol. Appl. Pharmacol.* **2013**, *267*, 30−40.
(10) Pryor, W. A.; Squadrito, G. L.; Friedman, M. The Cascade Mechanism to Explain Ozone Toxicity: The Role of Lipid Ozonation Products. *Free Radical Biol. Med.* **1995**, *19*, 935−941.
(11) Smith, N. L.; Wilson, A. L.; Gandhi, J.; Vatsia, S.; Khan, S. A. Ozone Therapy: An Overview of Pharmacodynamics, Current Research, and Clinical Utility. *Med. Gas Res.* **2017**, *7*, 212.
(12) Delgado-Roche, L.; Riera-Romo, M.; Mesta, F.; Hernández-Matos, Y.; Barrios, J. M.; Martínez-Sánchez, G.; Al-Dalaien, S. M. Medical Ozone Promotes Nrf2 Phosphorylation Reducing Oxidative Stress and Pro-Inflammatory Cytokines in Multiple Sclerosis Patients. *Eur. J. Pharmacol.* **2017**, *811*, 148−154.
(13) Farac, R. V.; Pizzolitto, A. C.; Tanomaru, J. M. G.; Morgental, R. D.; Lima, R. K. D. P.; Bonetti-Filho, I. Ex-Vivo Effect of Intracanal Medications Based on Ozone and Calcium Hydroxide in Root Canals Contaminated with Enterococcus Faecalis. *Braz. Dent. J.* **2013**, *24*, 103−106.
(14) Heß, S.; Gallert, C. Sensitivity of Antibiotic Resistant and Antibiotic Susceptible Escherichia Coli, Enterococcus and Staphylococcus Strains against Ozone. *J. Water Health* **2015**, *13*, 1020−1028.
(15) Rangel, K.; Cabral, F. O.; Lechuga, G. C.; Carvalho, J. P. R. S.; Villas-Bôas, M. H. S.; Midlej, V.; De-Simone, S. G. Potent Activity of a High Concentration of Chemical Ozone against Antibiotic-Resistant Bacteria. *Molecules* **2022**, *27*, 3998.
(16) Thanomsub, B.; Anupunpisit, V.; Chanphetch, S.; Watcharachaipong, T.; Poonkhum, R.; Srisukonth, C. Effects of Ozone Treatment on Cell Growth and Ultrastructural Changes in Bacteria. *J. Gen. Appl. Microbiol.* **2002**, *48*, 193−199.
(17) Mehraban, F.; Seyedarabi, A. Molecular Effects of Ozone on Amino Acids and Proteins, Especially Human Hemoglobin and Albumin, and the Need to Personalize Ozone Concentration in Major Ozone Autohemotherapy. *Crit. Rev. Clin. Lab. Sci.* **2023**, 1−16.
(18) Mehraban, F.; Seyedarabi, A.; Seraj, Z.; Ahmadian, S.; Poursasan, N.; Rayati, S.; Moosavi-Movahedi, A. A. Molecular Insights into the Effect of Ozone on Human Hemoglobin in Autohemotherapy: Highlighting the Importance of the Presence of Blood Antioxidants during Ozonation. *Int. J. Biol. Macromol.* **2018**, *119*, 1276−1285.
(19) Bocci, V.; Zanardi, I.; Travagli, V. Ozone: A New Therapeutic Agent in Vascular Diseases. *Am. J. Cardiovasc. Drugs* **2011**, *11*, 73−82.
(20) Briner, E. Accelerating Action of Ozone in the Autoxidation Processes. In *Ozone chemistry and technology*; Advances in Chemistry; 1959; Vol. *21*, pp. 28−184, DOI: 10.1021/ba-1959-0021.ch028.
(21) Seyedarabi, A.; Ariaeenejad, S.; Moosavi-Movahedi, A. A.; Rayati, S.; Poursasan, N.; Asiaie, N.; Seraj, Z.; Mehraban, F.; Seyedarabi, S. E. Novel X-Ray Sequences and Crystal Structures of Persian and Starry Sturgeon Methemoglobins: Highlighting the Role of Heme Pocket Waters in Causing Autoxidation. *Biochim. Biophys. Acta, Proteins Proteomics* **2019**, *1867*, 586−594.
(22) Tsuruga, M.; Shikama, K. Biphasic Nature in the Autoxidation Reaction of Human Oxyhemoglobin. *Biochim. Biophys. Acta, Protein Struct. Mol. Enzymol.* **1997**, *1337*, 96−104.
(23) Macdonald, V. W. B. T.-M. Measuring Relative Rates of Hemoglobin Oxidation and Denaturation. In *Hemoglobins Part B: Biochemical and Analytical Methods*; 1994; Vol. *231*, pp. 480−490, DOI: 10.1016/0076-6879(94)31031-9.
(24) Ladner, R. C.; Heidner, E. J.; Perutz, M. F. The Structure of Horse Methaemoglobin at 2.0 Å Resolution. *J. Mol. Biol.* **1977**, *114*, 385−413.
(25) Mansouri, A.; Winterhalter, K. H. Nonequivalence of Chains in Hemoglobin Oxidation and Oxygen Binding. Effect of Organic Phosphates. *Biochemistry* **1974**, *13*, 3311−3314.

(26) Takano, T. Structure of Myoglobin Refined at 2·0 Å Resolution: I. Crystallographic Refinement of Metmyoglobin from Sperm Whale. *J. Mol. Biol.* **1977**, *110*, 537−568.
(27) Liong, E. C.; Dou, Y.; Scott, E. E.; Olson, J. S.; Phillips, G. N. Waterproofing the Heme Pocket: ROLE OF PROXIMAL AMINO ACID SIDE CHAINS IN PREVENTING HEMIN LOSS FROM MYOGLOBIN*. *J. Biol. Chem.* **2001**, *276*, 9093−9100.
(28) Grinshtein, N.; Bamm, V. V.; Tsemakhovich, V. A.; Shaklai, N. Mechanism of Low-Density Lipoprotein Oxidation by Hemoglobin-Derived Iron. *Biochemistry* **2003**, *42*, 6977−6985.
(29) Cataldo, F. Ozone Degradation of Biological Macromolecules: Proteins, Hemoglobin, RNA, and DNA. *Ozone: Sci. Eng.* **2006**, *28*, 317−328.
(30) Mehraban, F.; Seyedarabi, A.; Ahmadian, S.; Mirzaaghaei, V.; Moosavi-Movahedi, A. A. Personalizing the Safe, Appropriate and Effective Concentration(s) of Ozone for a Non-Diabetic Individual and Four Type II Diabetic Patients in Autohemotherapy through Blood Hemoglobin Analysis. *J. Transl. Med.* **2019**, *17*, 227.
(31) Mehraban, F.; Rayati, S.; Mirzaaghaei, V.; Seyedarabi, A. Highlighting the Importance of Water Alkalinity Using Phosphate Buffer Diluted With Deionized, Double Distilled and Tap Water, in Lowering Oxidation Effects on Human Hemoglobin Ozonated at High Ozone Concentrations in Vitro. *Front. Mol. Biosci.* **2020**, *7*, No. 543960.
(32) Chan, W. K. M.; Faustman, C.; Yin, M.; Decker, E. A. Lipid Oxidation Induced by Oxymyoglobin and Metmyoglobin with Involvement of H2O2 and Superoxide Anion. *Meat Sci.* **1997**, *46*, 181−190.
(33) Baieth, H. E.-S. A.; Elashmawi, I. S. Influence of Ozone on the Rheological and Electrical Properties of Stored Human Blood. *J. Biomed. Res.* **2012**, *26*, 185−192.
(34) Pettersen, E. F.; Goddard, T. D.; Huang, C. C.; Couch, G. S.; Greenblatt, D. M.; Meng, E. C.; Ferrin, T. E. UCSF Chimera—A Visualization System for Exploratory Research and Analysis. *J. Comput. Chem.* **2004**, *25*, 1605−1612.
(35) Laskowski, R. A.; Swindells, M. B. LigPlot+: Multiple Ligand−Protein Interaction Diagrams for Drug Discovery. *J. Chem. Inf. Model.* **2011**, *51*, 2778−2786.
(36) Zeserson, E.; Goodgame, B.; Hess, J. D.; Schultz, K.; Hoon, C.; Lamb, K.; Maheshwari, V.; Johnson, S.; Papas, M.; Reed, J.; Breyer, M. Correlation of Venous Blood Gas and Pulse Oximetry with Arterial Blood Gas in the Undifferentiated Critically Ill Patient. *J. Intensive Care Med.* **2018**, *33*, 176−181.
(37) Rieser, T. M. Arterial and Venous Blood Gas Analyses. *Top. Companion Anim. Med.* **2013**, *28*, 86−90.
(38) Ghisaidoobe, A. B. T.; Chung, S. J. Intrinsic Tryptophan Fluorescence in the Detection and Analysis of Proteins: A Focus on Förster Resonance Energy Transfer Techniques. *Int. J. Mol. Sci.* **2014**, *15*, 22518−22538.
(39) Kelly, S. M.; Price, N. C. The Use of Circular Dichroism in the Investigation of Protein Structure and Function. *Curr. protein Pept. Sci.* **2000**, *1*, 349−384.
(40) Rogers, D. M.; Jasim, S. B.; Dyer, N. T.; Auvray, F.; Réfrégiers, M.; Hirst, J. D. Electronic Circular Dichroism Spectroscopy of Proteins. *Chem* **2019**, *5*, 2751−2774.
(41) Muñoz, G.; de Juan, A. PH- and Time-Dependent Hemoglobin Transitions: A Case Study for Process Modelling. *Anal. Chim. Acta* **2007**, *595*, 198−208.
(42) Nienhaus, K.; Nienhaus, G. U. Probing Heme Protein-Ligand Interactions by UV/Visible Absorption Spectroscopy. *Protein-Ligand Interactions: Methods and Applications* **2005**, 215−241.
(43) Kampf, C. J.; Liu, F.; Reinmuth-Selzle, K.; Berkemeier, T.; Meusel, H.; Shiraiwa, M.; Pöschl, U. Protein Cross-Linking and Oligomerization through Dityrosine Formation upon Exposure to Ozone. *Environ. Sci. Technol.* **2015**, *49*, 10859−10866.
(44) Carvalho, F. A. O.; Carvalho, J. W. P.; Santiago, P. S.; Tabak, M. Further Characterization of the Subunits of the Giant Extracellular Hemoglobin of Glossoscolex Paulistus (HbGp) by SDS-PAGE Electrophoresis and MALDI-TOF-MS. *Process Biochem.* **2011**, *46*, 2144−2151.
(45) Lorber, B.; Fischer, F.; Bailly, M.; Roy, H.; Kern, D. Protein Analysis by Dynamic Light Scattering: Methods and Techniques for Students. *Biochem. Mol. Biol. Educ.* **2012**, *40*, 372−382.
(46) Ostolska, I.; Wiśniewska, M. Application of the Zeta Potential Measurements to Explanation of Colloidal Cr2O3 Stability Mechanism in the Presence of the Ionic Polyamino Acids. *Colloid Polym. Sci.* **2014**, *292*, 2453−2464.
(47) Huang, Y.-X.; Wu, Z.-J.; Huang, B.-T.; Luo, M. Pathway and Mechanism of PH Dependent Human Hemoglobin Tetramer-Dimer-Monomer Dissociations. *PLoS One* **2013**, *8*, No. e81708.

https://doi.org/10.1021/acsomega.3c01288
ACS Omega 2023, 8, 20714−20729